Supporting Information

Predicted Mode of Binding to and Allosteric Modulation of the μ-Opioid Receptor by Kratom's Alkaloids with Reported Antinociception in Vivo

Yuchen Zhou,[1] Steven Ramsey,[1] Davide Provasi,[1] Amal El Daibani,[2,3] Kevin Appourchaux,[2,3] Soumen Chakraborty,[2,3] Abhijeet Kapoor,[1] Tao Che,[2,3] Susruta Majumdar,[2,3] and Marta Filizola[1,*]

[1]*Department of Pharmacological Sciences, Icahn School of Medicine at Mount Sinai, One Gustave L. Levy Place, Box 1677, New York, New York 10029-6574, United States*

[2]*Department of Anesthesiology, Washington University in St. Louis School of Medicine, St Louis, Missouri 63110, United States*

3Center for Clinical Pharmacology, St. Louis College of Pharmacy and Washington University School of Medicine, St. Louis, Missouri 63110, United States

Table S1. MOP residues that are most significantly contributing (> 2% flux) to the transfer entropy between the ligand-binding pocket and the intracellular region of the receptor. Residues that are common among all three systems are colored in red. Residues that are common between MG-bound and MP-bound MOP systems are colored in orange, those that are common between 7OH-bound and MP-bound MOP systems are colored in green, and those that are common between MG-bound and 7OH-bound MOP systems are colored in blue.

MG-bound MOP		7OH-bound MOP		MP-bound MOP	
Residues	Contribution (%)	Residues	Contribution (%)	Residues	Contribution (%)
T103(2.39)	11.60	L275(6.30)	19.39	W293(6.48)	24.95
C170(3.55)	11.12	T218(45.51)	11.18	P181(4.39)	18.73
P181(4.39)	9.04	N342(8.49)	10.94	L275(6.30)	15.98
A102(2.38)	8.85	K271(6.26)	10.61	I105(2.41)	13.19
I105(2.41)	8.80	E341(8.48)	10.04	L129(2.65)	8.89
I234(5.40)	7.62	T103(2.39)	10.02	T103(2.39)	8.61
T101(2.37)	7.07	R277(6.32)	8.67	F152(3.37)	8.45
D164(3.49)	7.03	P181(4.39)	8.58	I256(5.62)	7.27
L275(6.30)	6.98	R165(3.50)	7.72	V126(2.62)	6.77
F178(34.56)	6.79	R258(5.64)	7.55	R165(3.50)	6.63
A323(7.40)	6.65	M255(5.61)	7.16	T101(2.37)	6.11
N342(8.49)	6.62	Y149(3.34)	6.54	M255(5.61)	5.87
R165(3.50)	6.61	L259(5.65)	6.27	T97(12.48)	5.26
E341(8.48)	6.25	F152(3.37)	6.12	R182(4.40)	5.17
M255(5.61)	6.14	V262(5.68)	6.02	K100(12.51)	5.10
D340(8.47)	5.92	F221(EL2)	6.00	V262(5.68)	5.08
T180(4.38)	5.88	C140(3.25)	5.97	A102(2.38)	4.88
R182(4.40)	5.52	K260(5.66)	5.68	F237(5.43)	4.73
I256(5.62)	5.49	V143(3.28)	5.61	M99(12.50)	4.72
E229(5.35)	5.48	N274(6.29)	5.45	N183(4.41)	4.62
R258(5.64)	5.26	V300(6.55)	5.41	R277(6.32)	4.42
V126(2.62)	5.18	N150(3.35)	5.35	R258(5.64)	4.20
L324(7.41)	5.05	I71(1.35)	5.34	F289(6.44)	4.17
A184(4.42)	4.87	M99(12.50)	4.94	L257(5.63)	4.14
C235(5.41)	4.85	L257(5.63)	4.87	L259(5.65)	3.95
Y75(1.39)	4.85	D340(8.47)	4.82	C217(45.50)	3.92
C321(7.38)	4.62	T101(2.37)	4.40	N342(8.49)	3.80
G325(7.42)	4.47	I256(5.62)	4.37	A184(4.42)	3.67
Y326(7.43)	4.26	L129(2.65)	4.14	K271(6.26)	3.62
N183(4.41)	4.15	N104(2.40)	4.02	D340(8.47)	3.61

L257(5.63)	4.00	T120(2.56)	3.96	F178(34.56)	3.48
N104(2.40)	3.86	I146(3.31)	3.95	T180(4.38)	3.40
I238(5.44)	3.60	S261(5.67)	3.84	E341(8.48)	3.36
S125(2.61)	3.52	Y227(5.33)	3.82	N274(6.29)	3.29
I301(6.56)	3.46	T97(12.48)	3.60	C170(3.55)	3.19
L232(5.38)	3.40	R263(IL3)	3.43	S261(5.67)	3.09
T327(7.44)	3.35	L339(7.56)	3.30	F343(8.50)	3.08
I298(6.53)	3.29	D272(6.27)	3.18	N104(2.40)	2.87
R277(6.32)	3.19	K100(12.51)	3.04	L232(5.38)	2.78
A168(3.53)	3.12	W133(23.50)	3.01	T279(6.34)	2.76
L259(5.65)	3.10	L219(45.52)	2.96	Y149(3.34)	2.73
Y96(1.60)	3.06	K233(5.39)	2.92	Y336(7.53)	2.67
C346(8.53)	3.00	M264(IL3)	2.52	L339(7.56)	2.65
R179(34.57)	2.99	N230(5.36)	2.50	N150(3.35)	2.49
P172(34.50)	2.99	F343(8.50)	2.50	T120(2.56)	2.44
N274(6.29)	2.84	D216(45.49)	2.48	C346(8.53)	2.30
K100(12.51)	2.70	D164(3.49)	2.29	S125(2.61)	2.29
A175(34.53)	2.35	C170(3.55)	2.26	A240(5.46)	2.27
K260(5.66)	2.13	I105(2.41)	2.10	A168(3.53)	2.26
C292(6.47)	2.13	P172(34.50)	2.04	Y128(2.64)	2.25
K271(6.26)	2.12			D272(6.27)	2.17
L339(7.56)	2.05			P122(2.58)	2.15
I167(3.52)	2.01			R263(IL3)	2.14

Table S2. *Binding Pose Metadynamics* CompScore of the 3 top cluster representatives of MG, 7OH, and MP from docking at MOP. The best pose for each ligand, indicated by the lowest CompScore value, is highlighted in bold typeface.

Pose	MG		7OH		MP	
#1	0.64	(0.56, 2.2)	**-3.26**	**(-4.23, -3.59)**	**1.44**	**(1.1, 1.82)**
#2	**-3.26**	**(-3.81, -2.72)**	1.54	(1.02, 1.73)	3.04	(2.08, 4.33)
#3	2.65	(2.18, 3.26)	-1.14	(-2.82, -0.47)	2.27	(1.49, 3.49)

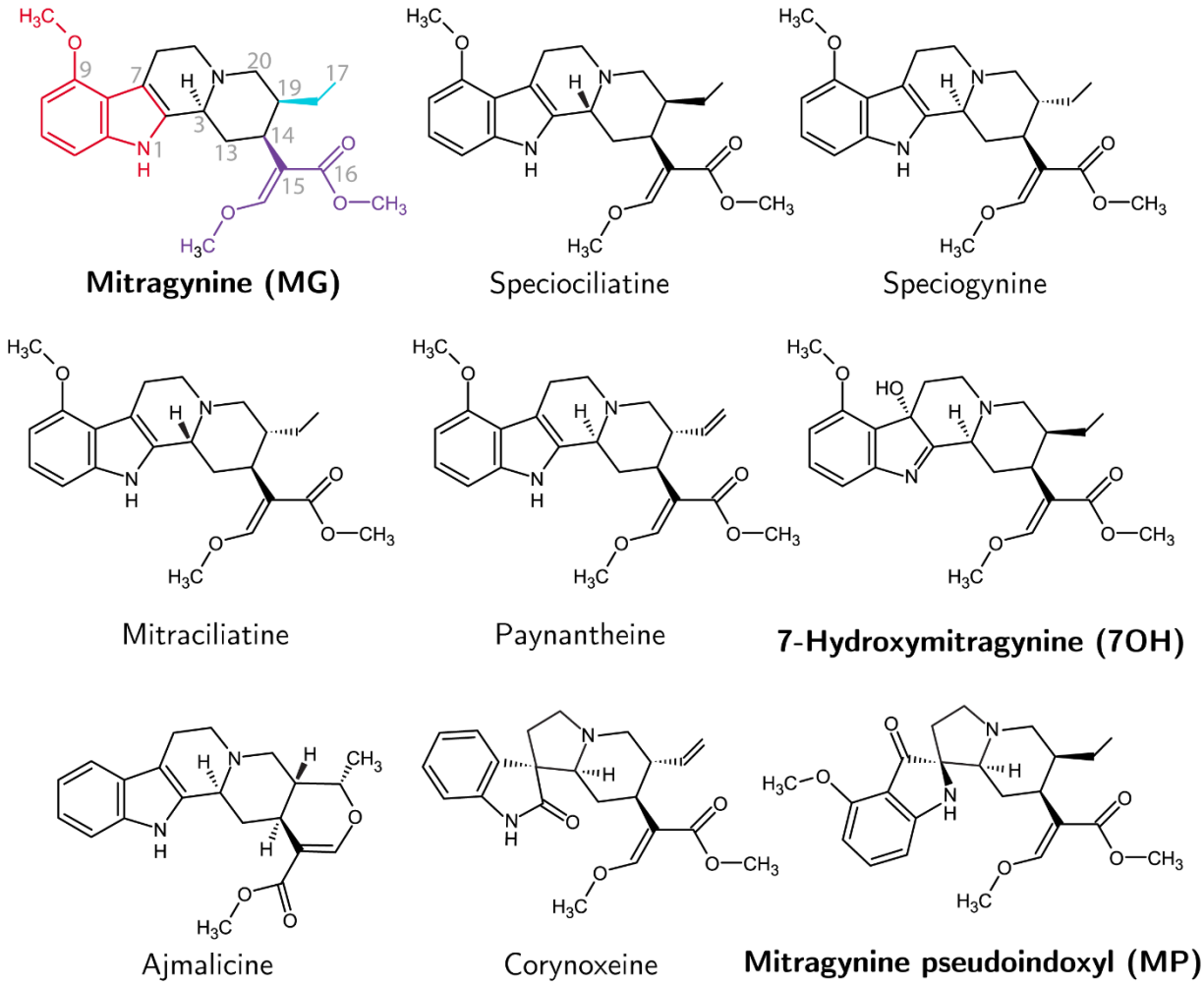

Figure S1. Structures of kratom alkaloids cited in this paper. Carbon atom numbering cited in the text is indicated on the mitragynine structure. Ethyl group at position C19, the β-methoxyacrylate moiety, and the methoxyindole group are indicated in cyan, purple, and red, respectively.

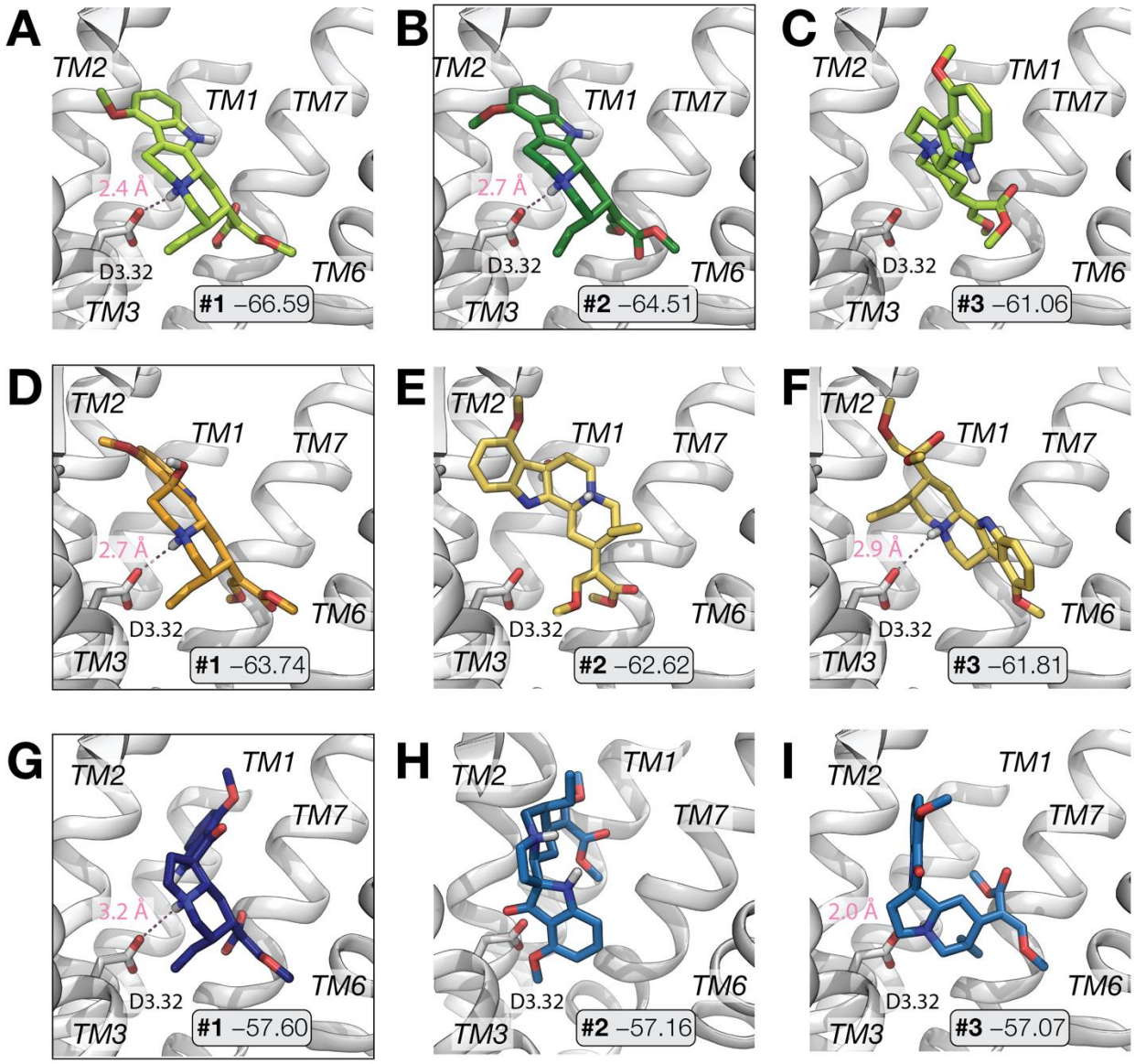

Figure S2. Binding poses and DOCK6.9 scores (in kcal/mol) for MG (poses #1-#3; A-C), 7OH (poses #1-#3; D-F), and MP (poses #1-#3; G-I). The top-ranked metadynamics-rescored poses selected for production simulations are indicated by a black box. The distance of the H-bond between Asp147$^{3.32}$ and the ligand's charged amine is indicated in pink when less than 3.5 Å. The MOP helices are shown in light grey cartoon representation. TM4 and TM5 are not shown for clarity.

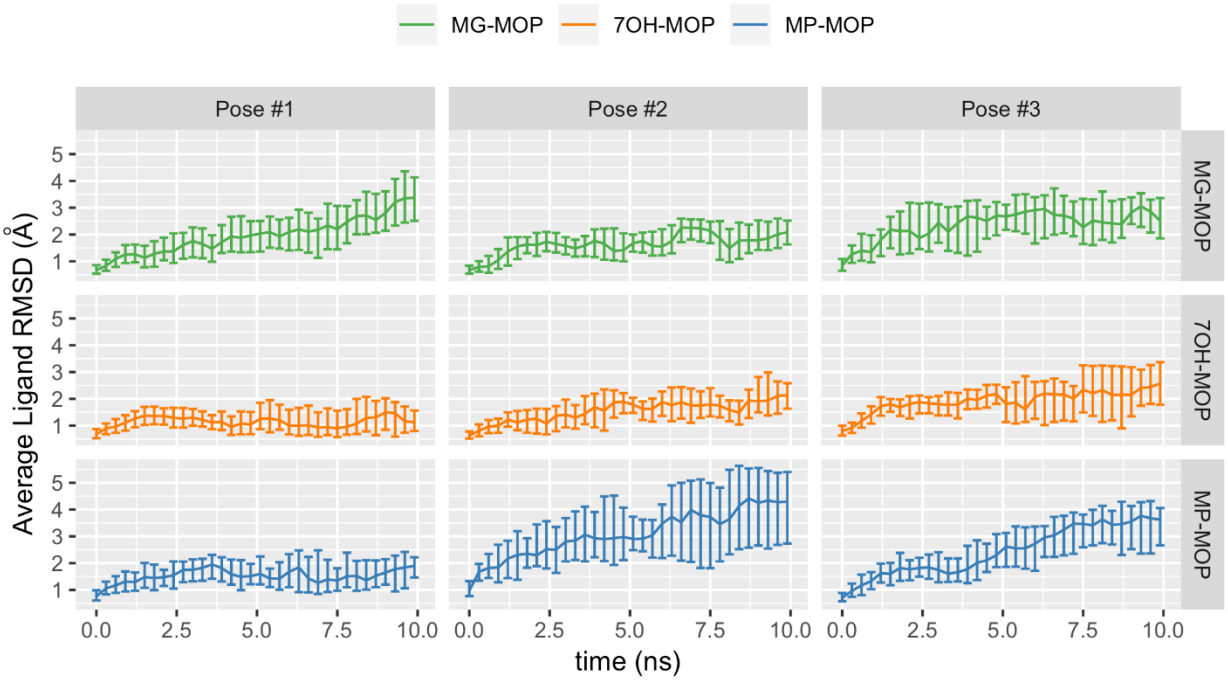

Figure S3. Time evolution of the RMSD of MG (green), 7OH (orange), and MP (blue) heavy atoms from their initial docking conformations calculated for each selected pose across the 10 independent metadynamics simulations used for CompScore ranking. Error bars denote the 25th and 75th percentiles.

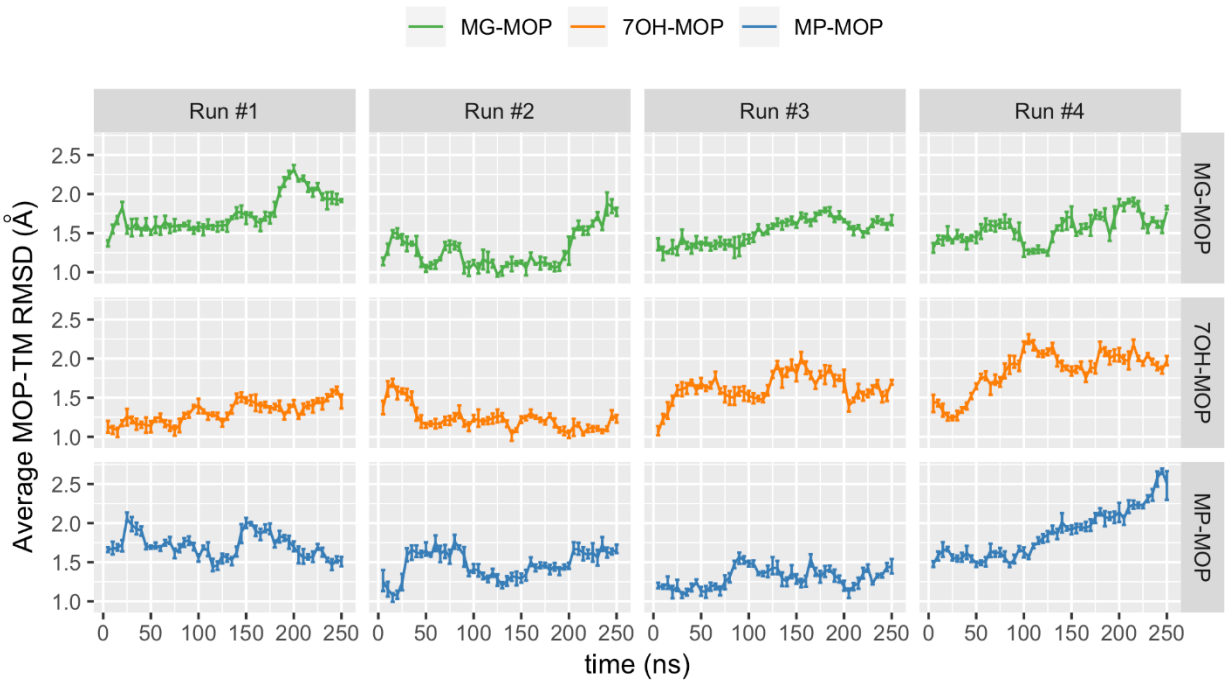

Figure S4. Time evolution of the RMSD of the alpha-carbons of the MG-bound (green), 7OH-bound (orange), and MP-bound (blue) MOP transmembrane region from the corresponding region in the 5C1M crystal structure, monitored during four 250 ns production simulations carried out for each ligand-MOP complex. RMSD is reported in bins of 5 ns as an average value with error bars denoting the 25th and 75th percentiles.

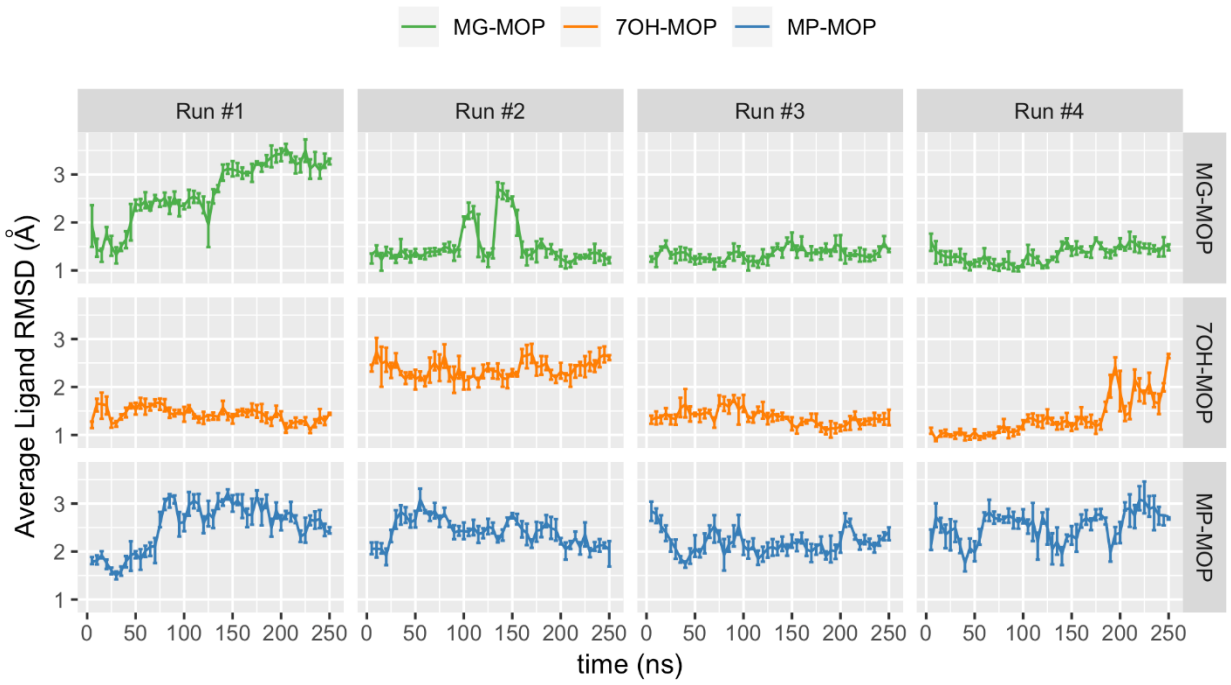

Figure S5. Time evolution of the RMSD of the heavy atoms of MG (green), 7OH (orange), and MP (blue) from those in the docked conformations, monitored after alignment of the protein TM alpha-carbon atoms and during four 250 ns production simulations carried out for each ligand-MOP complex. RMSD is reported in bins of 5 ns as an average value with error bars denoting the 25th and 75th percentiles.

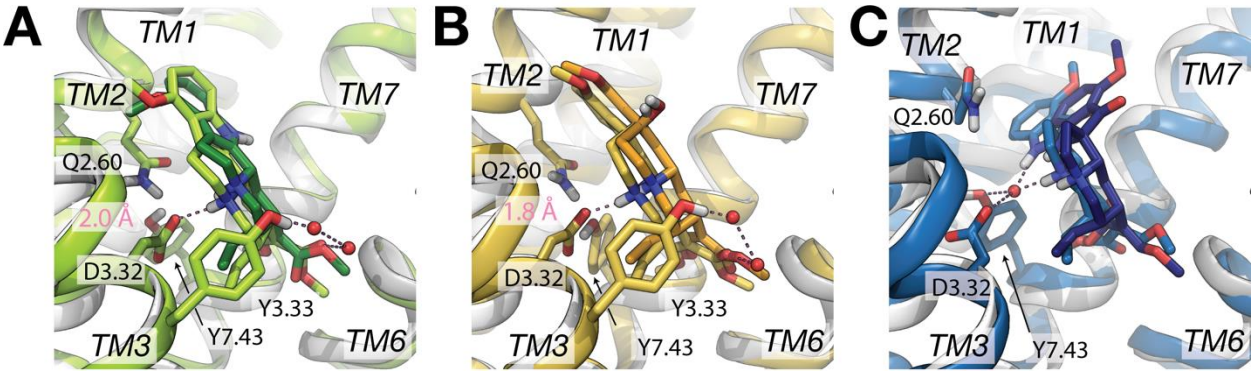

Figure S6. Representative binding conformations (light colors) of the largest MD simulation clusters obtained for (A) MG-MOP, (B) 7OH-MOP, and (C) MP-MOP overlapped onto their respective starting, docking conformations (dark colors). The MOP crystal structure corresponding to 5C1M is shown in gray as a reference. Direct H-bond distances between the ligand's charged amine and D3.32 in the MD clusters are shown for MG and 7OH. Red spheres indicate water molecules involved in high probability (>50%) interactions with both the ligand and the protein. Specifically, 2-water-mediated interactions connecting Y3.33 to the carbonyl group of the the β-methoxyacrylate moiety of MG or 7OH are indicated with dotted lines in panels (A) and (B), respectively, while 1-water-mediated interactions connecting D3.32 or Y7.43 to MP are indicated in panel (C).

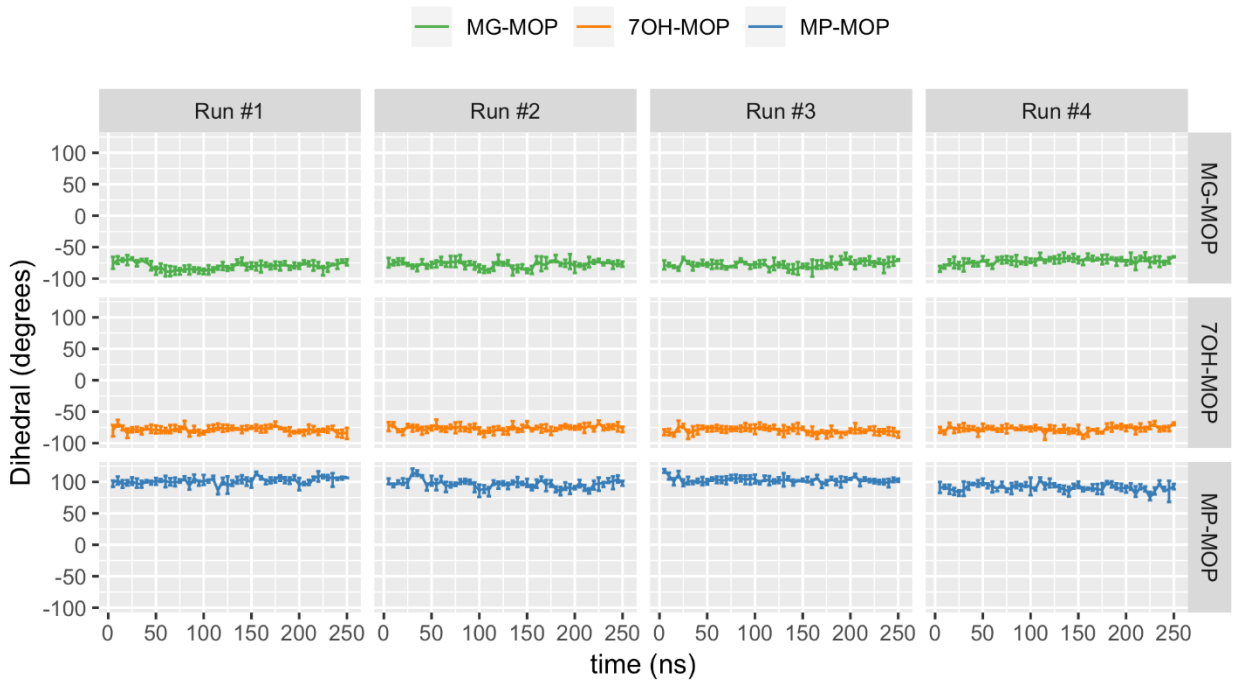

Figure S7. Time evolution of the C19-C14-C15-C16 dihedral angle (refer to the carbon numbering reported in Figure S1) of the β-methoxyacrylate moiety of MG (green), 7OH (orange), and MP (blue), monitored during four 250 ns production simulations carried out for each ligand-MOP complex. The value of the angle is reported in bins of 5 ns as an average value with error bars denoting the 25th and 75th percentiles.